Mem. S.A.It. Vol. , 1

Memorie della

Colour and stellar population gradients in galaxies

C. Tortora[1], N.R. Napolitano[2], V.F. Cardone[3], M. Capaccioli[4], P. Jetzer[1], and R. Molinaro[2]

[1] Universität Zürich, Institut für Theoretische Physik, Winterthurerstrasse 190, CH-8057, Zürich, Switzerland e-mail: ctortora@physik.uzh.ch
[2] INAF – Osservatorio Astronomico di Capodimonte, Salita Moiariello, 16, 80131 - Napoli, Italy
[3] Dipartimento di Fisica Generale A. Avogadro, Università di Torino and Istituto Nazionale di Fisica Nucleare - Sezione di Torino, Via Pietro Giuria 1, 10125 - Torino, Italy
[4] Dipartimento di Scienze Fisiche, Università di Napoli Federico II, Compl. Univ. Monte S. Angelo, 80126 - Napoli, Italy

Abstract. We discuss the colour, age and metallicity gradients in a wide sample of local SDSS early- and late-type galaxies. From the fitting of stellar population models we find that metallicity is the main driver of colour gradients and the age in the central regions is a dominant parameter which rules the scatter in both metallicity and age gradients. We find a consistency with independent observations and a set of simulations. From the comparison with simulations and theoretical considerations we are able to depict a general picture of a formation scenario.

Key words. galaxies : evolution – galaxies : elliptical and lenticular, cD.

1. Introduction

Different physical processes might rule the galaxies' properties at the global galaxy scale, or act at sub-galactic scales (e.g. the nuclear regions vs outskirts), such that they are expected to introduce a gradient of the main stellar properties with the radius that shall leave observational signatures in galaxy colours. In fact, color gradients (CGs) are efficient markers of the stellar properties variations within galaxies, in particular as they mirror the gradients of star ages and metallicities (Tortora et al. 2010a, T+10 hereafter). CGs are primarily a tool to discriminate the two broad formation scenarios (monolithic vs hierarchical), but more importantly they provide a deeper insight on the different mechanisms ruling the galaxy evolution. As these mechanisms depend on the galaxy mass scale, the widest mass (and luminosity) observational baseline is needed to remark the relative effectiveness of the different physical processes (such as merging, AGN, supernovae, stellar feedback, etc) and their correlation with the observed population gradients.

We will discuss the colour, age and metallicity gradients for a huge sample of local SDSS early- and late-type galaxies (ETGs and LTGs, hereafter) from Blanton et al. (2005b,

Send offprint requests to: C. Tortora

B+05 hereafter), and analyze the trends with mass. The observed trends are interpreted by means of quite different physical phenomena at the various mass scales. See T+10 for further details[1].

We assume a set of "single burst" synthetic stellar models from Bruzual & Charlot (2003), with age and metallicity (Z) free to vary. From the fitting to the observed colours we estimate the galaxy age, Z, and the stellar mass[2].

2. Colour gradients

We start from showing in Fig. 1 the results for the $g-i$ CGs as a function of stellar mass and velocity dispersion for the whole galaxy sample. The gradients as a function of velocity dispersion look negative almost everywhere. Although our sample does not include very massive galaxies ($M_* \gtrsim 10^{11.5}\,M_\odot$), our results seem to show a stable trend at the large mass scales, pointing to even shallower gradients. We note here that the smaller range shown by ∇_{g-i} as a function of σ_0 in the left panel of Fig. 1 is mainly due to the mix of the ETGs and LTGs. While, the correlation with stellar mass show that, starting from the massive/bright end, the CGs become steeper, with the steepest negative gradients corresponding to $M_* \sim 10^{10.3}\,M_\odot$. From there, the gradients invert the trend with luminosity and mass, becoming positive at $M_* \sim 10^{8.7}\,M_\odot$.

From Fig. 2, we see that LTGs show a monotonic decreasing trend, while a U-shaped function is found for ETGs with the gradients definitely decreasing with the mass for $M_* \lesssim 10^{10.3-10.5}\,M_\odot$, and a mildly increasing for larger mass values. This mass scale is

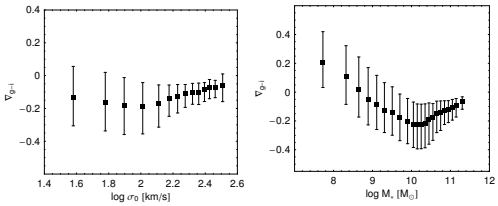

Fig. 1. ∇_{g-i} as a function of central velocity dispersion (left panel) and stellar mass (right panel) for the whole sample of galaxies. Medians and 25-75th quantiles of the sample distribution in each mass bin are shown.

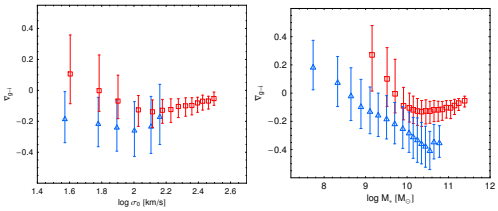

Fig. 2. ∇_{g-i} as a function of central velocity dispersion (left panel) and stellar mass (right panel) for ETGs (red symbols) and LTGs (blue symbols).

roughly compatible with the typical luminosity (and mass) scale for ETG dichotomy in the galaxy structural properties (Capaccioli et al. 1992) or for star-forming and passive systems (Kauffmann et al. 2003). Nevertheless, for a fixed stellar mass we observe that ETGs gradients are, on average, shallower than LTG ones. The same two-fold trend is shown for ETGs gradients as function of the velocity dispersion, while no trend is observed for LTGs gradients.

3. Age and metallicity gradients

As shown in Fig. 3, for LTGs the ∇_{age} is about zero both with mass (and with σ_0, see T+10), strongly suggesting that CGs should not depend on age gradients of the galaxy stellar population. Actually, ∇_Z is instead strongly dependent on M_*, with the lowest metallicity gradients (~ -1) at the largest masses. ETG age gradients seem basically featureless when plotted against σ_0 where we find $\nabla_{age} > 0$ with typical median values of $\nabla_{age} \sim 0.2$. On

[1] We have used the structural parameters given by B+05 to derive the color profile $(X-Y)(R)$ of each galaxy as the differences between the (logarithmic) surface brightness measurements in the two bands, X and Y. The CG is defined as the angular coefficient of the relation $X-Y$ vs $\log R/R_{\rm eff}$, where $R_{\rm eff}$ is the effective radius.

[2] We define the age and metallicity gradients as $\nabla_{age} = \log[age_2/age_1]$ and $\nabla_Z = \log[Z_2/Z_1]$, where (age_i, Z_i) with $i = 1, 2$ are the estimated age and metallicity at $0.1R_{\rm eff}$ and $R_{\rm eff}$, respectively.

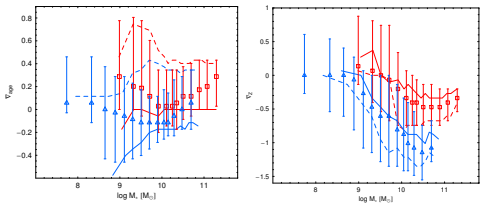

Fig. 3. Age (left) and metallicity (right) gradients as a function of stellar mass. The symbols are as in Fig. 2. Solid and dashed lines are for galaxies with central stellar populations older and younger than 6 Gyr, respectively.

the other hand, the metallicity gradients show some features with ∇_Z decreasing for $\log\sigma_0 \lesssim 2.2$ km/s, and increasing for larger velocity dispersion, reaching the shallowest values (~ -0.2) at $\log\sigma_0 \gtrsim 2.4$ km/s and at the very low σ_0 (i.e. $\log\sigma_0 < 1.8$ km/s) where $\nabla_Z \sim 0$. This peculiar trend is mirrored by a similar dependence on the stellar mass. This two-fold behaviour is also significant when we plot ∇_{age} as a function of the stellar mass: ∇_{age} decreases at $\log M_* \lesssim 10.3 - 10.5$, and increases in more massive systems. We have also found that ∇_{age} and ∇_Z strongly depend on galaxy age: in particular, if we separate the sample in systems with older and younger than 6 Gyr central stars, we obtain different age and metallicity gradient trends as shown in Fig. 3. Older systems have gradients which are shallower than younger (in particular for ETGs) and bracket the average trend of the whole samples.

In the left panel of Fig. 4 we proceed to a more detailed comparison of our findings with a set of literature works which make use of a more sophisticated analysis, although usually associated to smaller samples (e.g. Rawle et al. 2009, Spolaor et al. 2009). In particular, we concentrate on the ETG sample. When considering objects with $age_1 > 6$ Gyr, the agreement with the other studies (generally dealing with old systems) is remarkably good.

4. Discussion and conclusions

We have found some peculiar trends for CGs as a function of stellar mass, which are mainly driven by metallicity gradients, although age gradients have a not negligible role. ETGs, have gradients which are null at $\log M_* \sim 9.5$ and become steeper at $\log M_* \sim 10.5$, where the trend get inverted and tend to be shallower at very large masses. LTGs have null colour and metallicity gradients at $\log M_* \sim 8$, which steepen with stellar mass and at fixed mass metallicity gradients are steeper than the ones in ETGs. The scatter in gradients is driven by the central galaxy age, since centrally older (younger) systems are found to have shallower (steeper) metallicity gradients.

From the comparison with a set of simulations, which rely on different physical phenomena (e.g., see for ETGs right panel in Fig. 4), we are able to point out the main physical phenomena at different mass scales. Our results seem to support the idea that the metallicity trend versus the stellar mass for LTGs is mainly driven by the interplay of gas inflow and winds from supernovae and evolved stars (Kobayashi 2004). These processes tend to increase the central metallicity and prevent the enrichment of the outer regions. Therefore more massive systems have on average larger central metallicities which correspond to steeper negative gradients. Low mass ETGs show the same correlation (see also the results from the simulation in Tortora et al. 2010b), which suggest that these systems might experience similar phenomena as LTGs (see the comparison with the different supernovae feedback recipes in Fig. 4). Moreover, the absolute value of ∇_Z of ETGs is lower than for the LTGs, probably as a consequence of the dilution of the gradient due to the higher-density environment where ETGs generally are located. At very low masses ($M_* \lesssim 10^{9.5}\,M_\odot$ and $\log\sigma_c \lesssim 1.8$ km/s) the ∇_Z turns to even positive values, which are compatible with the expanding shell model from Mori et al. (1997). At larger masses, the shallow metallicity gradients of ETGs suggest that these have experienced merging (at a rate that could increase as a function of the stellar mass) which have diluted the ∇_Z. Such events might have taken place in earlier phases of the galaxy evolution, as indicated by the presence of null age gradients in old systems (not shown here, but see Bekki & Shioya 1999, Kobayashi 2004, Hopkins et al. 2009a).

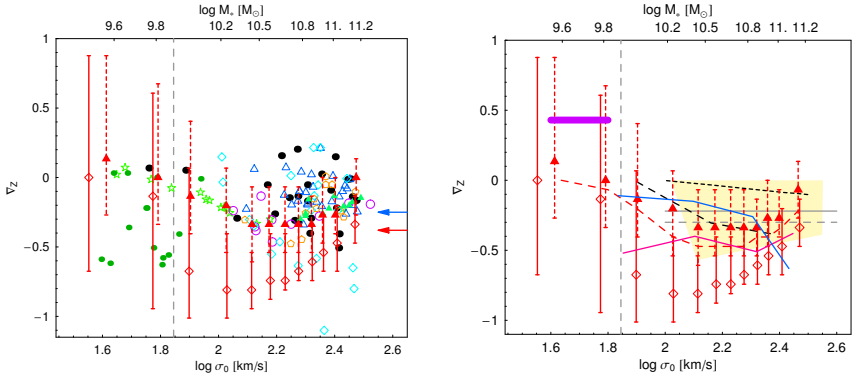

Fig. 4. *Left.* Metallicity gradients versus a set of observations (see T+10 for further details). *Right.* Metallicity gradients versus simulations. The predictions from merging models in Bekki & Shioya (1999) are shown as short dashed line, dissipative collapse models in Kawata & Gibson (2003) as long dashed line, the remnants of major-mergings between gas-rich disk galaxies in Hopkins et al. (2009a) as yellow shaded region, the typical gradient for major (continue gray line) and non-major (dashed gray line) mergings in Kobayashi (2004). The violet thick line shows the predictions as in the simulation of Mori et al. (1997); blue and pink lines are the result from the chemo-dynamical model in Kawata (2001), respectively for strong and weak supernovae feedback models. Triangles with dashed bars and boxes with continue bars are for galaxies centrally older and younger than 6 Gyr; in the right panel the dashed line is the median trend for all the ETG sample.

While, systems with younger cores are expected to show positive gradients (as found in Hopkins et al. (2009a)). After the initial gas rich-merging events that might produce both a larger central metallicity and a positive age gradient (Kobayashi 2004), subsequent gas poor-merging may dilute the positive age gradient with time as well as make the metallicity gradients to flatten out (Hopkins et al. 2009a). However, a further mechanism that may act to produce the shallower (or almost null) color and metallicity gradients in old massive ETGs, with $M_* \gtrsim 10^{11}\,M_\odot$ and $\log\sigma_0 \gtrsim 2.4$ (Fig. 4), might be due to the strong quasar feedback at high redshift (Tortora et al. 2009), while steeper metallicity gradients at lower masses could be linked to less efficient AGNs.

Acknowledgements. CT is supported by the Swiss National Science Foundation.

References

Blanton M. R. et al. 2005, AJ, 129, 2562 (B+05)
Bekki K., & Shioya Y. 1999, ApJ, 513, 108
Bruzual A. G. & Charlot S. 2003, MNRAS, 344, 1000
Capaccioli M., Caon N. & D'Onofrio M. 1992, MNRAS, 259, 323
Chabrier G. 2001, ApJ, 554, 1274
Dekel A. & Birnboim Y. 2006, MNRAS, 368, 2
Hopkins P. F. et al. 2009, ApJS, 181, 135
Kauffmann G. et al. 2003, MNRAS, 341, 54
Kawata D. 2001, ApJ, 558, 598
Kawata D. & Gibson B. K. 2003, MNRAS, 340, 908
Kobayashi C. 2004, MNRAS, 347, 740
Mori M. et al. 1997, ApJ, 478, 21
Rawle T.D., Smith R.J. & Lucey J.R. 2010, MNRAS, 401, 852
Spolaor M. et al. 2009, ApJ, 691, 138
Tortora C. et al. 2009, MNRAS, 396, 61
Tortora C. et al. 2010a, MNRAS, 407, 144 (T+10)
Tortora C. et al. 2010b, arXiv:1009.2500